Stringent limits on quark star masses due to the chiral transition temperature

A. Peshier[a], B. Kämpfer[b], G. Soff[c]
[a] *Department of Physics, Brookhaven National Laboratory, Upton, NY 11973, USA*
[b] *Forschungszentrum Rossendorf, PF 510119, 01314 Dresden, Germany*
[c] *Institut für Theoretische Physik, TU Dresden, 01062 Dresden, Germany*

Recent finite-temperature QCD lattice data are analyzed within a quasiparticle model, and extrapolated to nonzero chemical potential. Determined by the chiral transition temperature, the resulting equation of state of charge neutral, β-stable deconfined matter limits the mass and the size of quark stars.

Key Words: deconfined matter, quark stars
PACS number(s): 24.85.+p, 12.38.Mh, 21.65.+f, 26.60.+c

Soon after the discovery of quarks and gluons as the constituents of hadrons, the possible existence of quark cores in neutron stars has been conjectured [1]. Even before establishing quantum chromodynamics (QCD) as fundamental theory of strong interaction, the notion of quark matter in stars had been introduced by various authors [2]. Since that time many investigations have been performed to elucidate various consequences of this hypothesis. As one of the most fascinating conjectures, the existence of self-bound quark matter [3] and pure quark stars (as surveyed in [4]) was proposed. Other investigations are devoted to rapidly rotating quark stars [5], the cooling behavior of neutron stars with quark cores, and the mass-radius relation which is now becoming accessible to observation. If star matter exhibits a strongly first-order phase transition above nuclear density, a third stable family [6] of ultra-dense, cold stars can appear beyond the branches of white dwarfs and ordinary neutron stars, thus creating so-called twin stars. The necessary discontinuity in the equation of state (EoS) may be realized in nature at the chiral transition [7], but also other phase changes of nuclear matter may allow for twin stars [8]. The transition of a neutron star to the denser configuration, triggered e.g. by accretion, can be accompanied by an ejection of the outermost layers [9]. This may result in specific supernova events [8,10].

While different scenarios for these phenomena have been explored, most studies suffer from uncertainties of the EoS of strongly interacting matter. Predictions of the hadronic EoS, which can be adjusted to properties of nuclear matter, become increasingly model dependent when extrapolated above the nuclear saturation density. For deconfined matter, which we will consider in the following, the bag model EoS is often applied [1], which is, however, in conflict with thermodynamic QCD lattice data. Improved approaches take into account medium modifications of the quark masses [11] or rely on perturbation theory [12], but also introduce *a priori* undetermined model parameters.

Here we are going to describe deconfined matter within a quasiparticle picture [13,14]. The approach is tested in the nonperturbative regime by comparison to finite-temperature QCD lattice data, which completely fixes the intrinsic parameters. The model yields in a straightforward way the EoS at finite chemical potential and vanishing temperature, which is then employed to calculate bulk properties of quark stars.

Our starting point is the thermodynamic potential in the form $p(T,\mu) = \sum_i p_i - B(\Pi_j^*)$, where the contribution $p_i(T,\mu_i(\mu);m_i^2)$ of the thermodynamically relevant partons is given by the pressure of an ideal Bose or Fermi gas of quasiparticles with mass squared $m_i^2 = m_{0,i}^2 + \Pi_i^*$. $m_{0,i}$ is the rest mass of parton species i, and Π_i^* its asymptotic self-energy at the light cone (depending on the temperature T and the chemical potential μ). Perturbatively, this ansatz is motivated by the fact that in the interacting system the position of the poles of the transverse gluon propagator and the quark particle-excitation is, for the dominating hard momenta of the order T, μ, described approximately by mass shells. The longitudinal gluon modes and the quark hole-excitations, on the other hand, are overdamped in this region of the phase space. The function $B(\Pi_j^*)$ is determined from a thermodynamical self-consistency condition, via $\partial B/\partial\Pi_j^* = \partial p_j(T,\mu_j;m_j^2)/\partial m_j^2$.

This phenomenological approach reproduces the leading order perturbative result for the QCD pressure [14]. Since it partly resums terms of higher order, it can be supposed to be applicable at larger coupling strength. (This assertion was also made in Refs. [15] where the pressure or the entropy have been approximated by resumming the hard thermal loop self-energies.) Indeed, parameterizing the effective coupling by

$$G^2(T,\mu=0) = \frac{48\pi^2}{(33-2N_f)\ln\left(\frac{T+T_s}{T_c/\lambda}\right)^2}\,, \qquad (1)$$

finite-temperature QCD lattice data can be reproduced quantitatively, even in the close vicinity of the chiral transition temperature T_c, by adjusting T_s and λ as demonstrated in [13,14] for $N_f = 2$ and 4 light flavors, and in the quenched limit. Based on that, only estimates could be provided for the relevant case of three quark flavors with physical masses. Now, the predictions of the quasiparticle model can be considerably refined by systematically analyzing the recent lattice calculations [16] with

$N_f = 2, 3$ and $N_f = 2+1$. First of all, we emphasize the fact that the pressure, as a function of T/T_c and scaled by the free value, displays a striking universal behavior for different numbers of flavors [17]. This observation supports the proposed quasiparticle description.

In Ref. [16], the pressure $p(T)$ has been calculated on the lattice for two and three flavors with a quark (rest) mass $m^{\rm latt} = 0.4\,T$. These data can be reproduced by the quasiparticle model assuming either $m_{0,q} = 0.4\,T$ (fit 1 in Fig. 1a for $N_f = 2$) or $m_{0,q} = 0$ (fit 2); it naturally appears that the first option yields a slightly better fit. To estimate the effect of the temperature dependent quark mass $m^{\rm latt}$, we also calculated the pressure within the quasiparticle model assuming $m_{0,q} = 0$ and with λ and T_s from fit 1 (dotted line in Fig. 1a). The resulting variation of the order of 5% is within the uncertainty of the lattice data. To extrapolate the lattice data to the chiral limit, and to correct for finite size effects, it has been suggested in [16] to scale, for $2T_c \lesssim T \lesssim 4T_c$, the 'raw' data by a factor of 1.15. Assuming, as a conservative estimate, the validity of this extrapolation also for $T_c \lesssim T \lesssim 2T_c$ (as relevant below), it can be described in that interval with the parameters of fit 3. For larger temperatures, this fit is still within the estimated errors. The data for $N_f = 3$ are analyzed correspondingly, and the fit parameters are summarized in Table 1.

Encouraged by the convincing agreement of the quasiparticle model with the finite-temperature lattice data in the nonperturbative regime, it can be further extended to nonzero chemical potential which is not yet accessible to lattice calculations. This only assumes that the underlying quasiparticle structure does not change[1]. As shown in [14], Maxwell's relation imposes a partial differential flow equation for the effective coupling $G^2(T,\mu)$, which allows to calculate the pressure in parts of the T, μ plane if the coupling is known at finite T and $\mu = 0$. From the pressure p, the entropy and particle densities s and n follow by differentiating with respect to T and μ, respectively, and the energy density is obtained by $e = sT + n\mu - p$.

The above quasiparticle fits in which $m_{0,q}$ do not depend on T are mapped to finite quark chemical potential $\mu_q = \mu$ and to zero temperature. The difference of 15% between the fits of the 'raw' lattice data and the estimated continuum extrapolation is also apparent at $\mu \neq 0$. Remarkably, however, the relation $e(p)$ at $T = 0$ turns out to be rather similar for both fits. In particular, in both cases the energy densities at vanishing pressure are approximately equal. For $p \lesssim 15\,T_c^4$, both curves can be parameterized within 2% accuracy by a linear function

[1]For the equation of state, the phenomenon of color superconductivity plays a less important role since it occurs on the Fermi surface. The effect is of the order $(\Delta/\mu)^2$, where the gap Δ is small compared to μ [18].

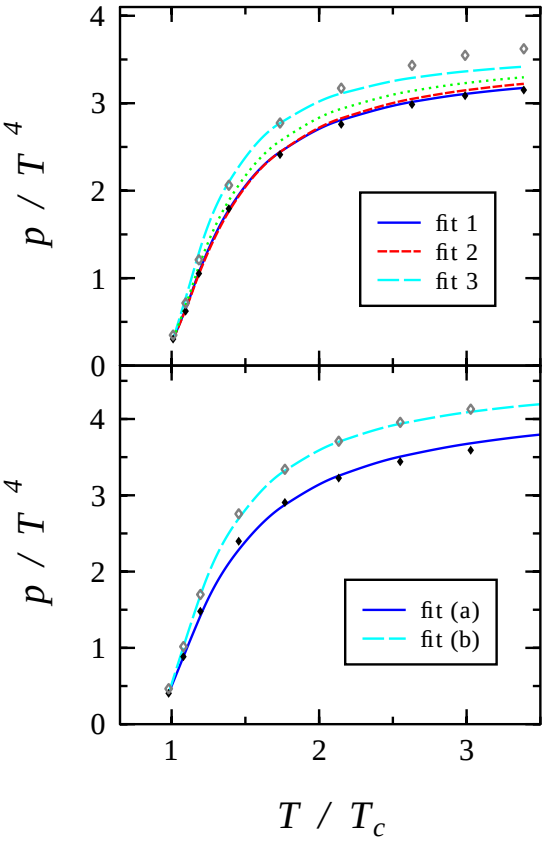

FIG. 1. The pressure for $N_f = 2$ (upper panel) and 2+1 (lower panel) at $\mu = 0$. The full symbols represent the lattice data [16], the open symbols are estimates for the continuum extrapolation. The quasiparticle fits and the dotted curve are explained in the text. The parameters $[\lambda, -T_s/T_c]$ for $N_f = 2$ are according to Table 1, and [3.5, 0.60] for fit (a) and [6.6, 0.78] for fit (b), respectively.

$$e(p) = 4\tilde{B} + \alpha p\,. \qquad (2)$$

The parameter $\tilde{B}$ is related to the bag constant in the bag model EoS, while a slope parameter α different from $\alpha_{\rm bag} = 3$ indicates nontrivial interaction effects. For the $N_f = 2$ case we find $4\tilde{B}_{[2]} \approx 19\,T_c^4$ and $\alpha_{[2]} \approx 3.4\ldots3.7$ (the larger value describes fit 2, the smaller one fit 3). For $N_f = 3$ we obtain $4\tilde{B}_{[3]} \approx 15\ldots16.5\,T_c^4$ and $\alpha_{[3]} \approx 3.4\ldots3.8$. The parameters are approximately equal for $N_f = 2$ and $N_f = 3$, which is, given the aforementioned universality of the scaled pressure for different numbers of flavors, not unexpected. Nonetheless, we emphasize again that in both cases the EoS at $T = 0$ in the form (2) is to a noteworthy degree insensitive (in contrast to the model parameters λ and T_s) to the remaining uncertainties of the lattice data.

With these remarks in mind, we turn to the discussion of the 2+1 flavor case. The lattice calculation [16] assumed $m_l^{\rm latt} = 0.4\,T$ for the light flavors, and $m_h^{\rm latt} = T$ for the heavy one. As shown in fit (a) in Fig. 1b, the data can be described in the quasiparticle model assuming the

same temperature dependent quark rest masses as on the lattice. For an estimate of the continuum result and in order to extrapolate to physical quark masses, we scale the lattice data again by a factor of 1.15 (motivated by the universality of the pressure for different flavor numbers and by the observed weak dependence on the quark rest masses). The scaled data can be reproduced by the quasiparticle model assuming $m_{0,l} = 0$ for the light flavors $l = u, d$, and $m_{0,s} = T_c$ for the strange flavor, see fit (b) in Fig 1b.

We now apply our model, with the parameters of fit (b), for the case of neutral quark matter in β equilibrium with leptons. The contribution of the leptons is approximated by a free electron gas, so the chemical potentials are related by $\mu = \mu_{d,s} = \mu_u + \mu_e$. The electron chemical potential $\mu_e(\mu)$ is determined by the requirement of electric neutrality. The pressure, as well as the quark and energy densities at $T = 0$, are depicted in Fig. 2. (With respect to [19] we mention that these results are not sensitive to the lepton component.)

The pressure of the deconfined phase vanishes at a chemical potential $\mu_c \approx 3.5\, T_c$, which provides a lower bound for the transition to the chirally broken phase. Lattice calculations [20] determine $T_c \approx 150 \ldots 170\,\mathrm{MeV}$. The uncertainty has, apart from the scaling, only a marginal effect on the thermodynamic properties shown in Fig. 2. Assuming $T_c = 160\,\mathrm{MeV}$ in the following, the net quark density n_q at $\mu_c = 556\,\mathrm{MeV}$ is approximately five times the quark density $\rho_0 = 3 \cdot 0.17/\mathrm{fm}^3$ in nuclear matter. This corresponds to an energy per baryonic degree of freedom of about 1.6 GeV. Consequently, strange quark matter is not stable according to our model. On the other hand, the value of $n_q(\mu_c)$ imposes a restriction on the EoS of hadronic matter, which still exhibits large theoretical uncertainties for higher densities.

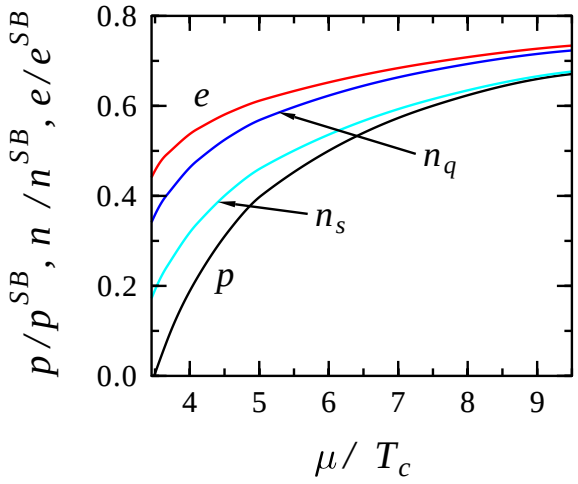

FIG. 2. The pressure, the strange and the net quark density, and the energy density for neutral and β-stable deconfined matter at $T = 0$, scaled by the Stefan-Boltzmann limits, where all masses can be neglected and μ_e vanishes.

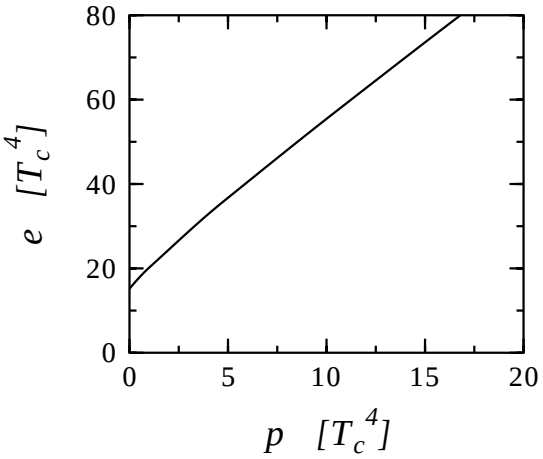

FIG. 3. The relation $e(p)$ from Fig. 2.

The relation $e(p)$ can again be parameterized by the linear function (2) (see Fig. 3) with $\alpha \approx 3.8$ and $\tilde{B}^{1/4} \approx 228\,\mathrm{MeV}$, which is considerably larger than the typical value of 145 MeV often used in the bag model.

It is interesting to compare our results to those of the perturbative approach [12], where also an almost linear relation $e(p)$ was found. For the choice of the renormalization scale $\bar{\Lambda} = 2\mu$, an effective bag constant $\approx 210\,\mathrm{MeV}$ (at $\alpha = 3$ fixed) and similar quark densities were obtained despite of a somewhat smaller value of μ_c.

The structure of nonrotating stars is determined by the Tolman-Oppenheimer-Volkov (TOV) equation (cf. [5]), in which the EoS of the star matter enters only in the form $e(p)$. In the following, we use the above results and consider stars composed entirely of neutral β-stable deconfined matter. We first recall a property of the TOV equation: If e and p are scaled by a factor of κ, the mass and length scales change by a factor of $\kappa^{-1/2}$. With the EoS (2), therefore, the mass and radius of the star are $\propto \tilde{B}^{-1/2}$ [3]. Increasing values of α lead to a softening of the EoS, which results in a larger pressure gradient in the star and to more compact configurations.

The mass-radius relation according to our EoS is shown in Fig. 4. Compared to results based on the conventional bag model EoS, which predict a maximum mass up to $1.5\, M_{\mathrm{sun}}$ and a corresponding radius $R \approx 10\,\mathrm{km}$ similar to the bulk properties of neutron stars, we find configurations which are smaller and lighter by, approximately, a factor of two (rotational effects may increase the maximum mass up to 30% [5]). This general statement is robust in our approach. The main effect is due to the large value of $\tilde{B}$, whereas the change $\alpha = 3 \to 3.8$ reduces the maximum mass and radius only by about 15%.

As pointed out in Refs. [6,8,12], an EoS allowing for a strong first-order transition to hadronic matter, as ours, can lead to a second stable branch in the mass-radius relation nearby the neutron star peak, thus permitting twin stars. These features, however, are sensitive to

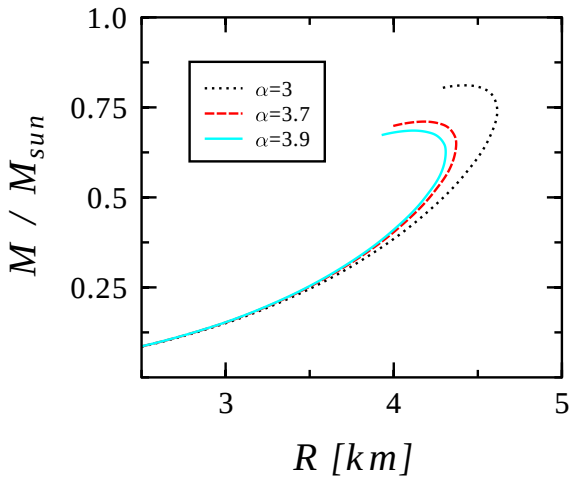

FIG. 4. The mass-radius relation of quark stars for the EoS (2) with $\tilde{B}^{1/4} = 228\,\mathrm{MeV}$ and parameters α around the fitted value. Left to the maximum mass, the upper branches become unstable.

details of the hadronic EoS and of the phase transition and deserve separate investigations.

In summary, our quasiparticle analysis of recent finite-temperature QCD lattice data [16] allows to predict the EoS at nonzero chemical potential. At $T = 0$, the relation $e(p)$ is found to be almost linear and insensitive to the remaining uncertainties of the lattice data. For QCD with physical quark masses, the resulting energy densities are large and exclude self-bound quark nuggets or strangelets. We find stringent limits on the mass and the size of strange quark stars: Assuming $T_c = 160\,\mathrm{MeV}$, the estimated maximum mass is $M_{\max} \approx 0.7\,M_{\mathrm{sun}}$, with a corresponding radius of $R_{\max} < 5\,\mathrm{km}$; these values scale as T_c^{-2}. Such small but dense objects are of interest with respect to MACHO events [12,21].

Useful discussions with D. Blaschke, J. Engels, E. Fraga, E. Grosse, F. Karsch, R. Pisarski, J. Schaffner-Bielich, F. Thielemann, and F. Weber are gratefully acknowledged. The work is supported by the grant BMBF 06DR921. A.P. is supported by DOE under grant DE-AC02-98CH10886 and by the A.-v.-Humboldt foundation (Feodor-Lynen program).

[1] J.C. Collins, M.J. Perry, Phys. Rev. Lett. **30**, 1353 (1975); G. Baym, S.A. Chin, Phys. Lett. B **62**, 241 (1976); B.D. Keister, L.S. Kisslinger, Phys. Lett. B **64**, 117 (1976); G. Chapline, M. Nauenberg, Phys. Rev. D **16**, 450 (1977); B.A. Freeman, L.D. McLerran, Phys. Rev. D **17**, 1109 (1978) and references therein.

[2] D. Iwanenkow, D.E. Kurtgelaidze, Nuovo Cimento Lett. **2**, 13 (1969); N. Itoh, Prog. Theor. Phys. **44**, 291 (1970).

[3] A.R. Bodmer, Phys. Rev. D **4**, 1601 (1971); E. Witten, Phys. Rev. D **30**, 272 (1984); J. Schaffner-Bielich, C. Greiner, A. Diener, H. Stöcker, Phys. Rev. C **55**, 3038 (1997).

[4] F. Weber, J. Phys. G **27**, 465c (2001).

[5] N.K. Glendenning, *Compact Stars*, Springer-Verlag, New York 1997; F. Weber, *Pulsars as astrophysical laboratories for nuclear and particle physics*, Bristol, UK, IOP, 1999; H. Heiselberg, M. Hjorth-Jensen, Phys. Rep. **328**, 237 (2000).

[6] U.H. Gerlach, Phys. Rev **172**, 1325 (1968); R.L. Bowers, A.M. Gleeson, R.D. Pedigo, Astrophys. J. **213**, 840 (1977); B. Kämpfer, Phys. Lett. B **101**, 366 (1981); J. Phys. A **14**, L471 (1981); L. Lindblom, Phys. Rev. D **58**, 024008 (1998).

[7] N.K. Glendenning, C. Kettner, Astron. Astrophys. **353**, L9 (2000).

[8] J. Schaffner-Bielich, M. Hanauske, H. Stöcker, W. Greiner, astro-ph/0005490.

[9] B. Kämpfer, Phys. Lett. B **153**, 121 (1985); Astrophys. Sp. Sci. **93**, 185 (1983).

[10] H.J. Haubold, B. Kämpfer, A.V. Senatorov, D.N. Voskresensky, Astron. Astrophys. **191**, L22 (1988).

[11] K. Schertler, C. Greiner, J. Schaffner-Bielich, M.H. Thoma, Nucl. Phys. A **677**, 463 (2000).

[12] E. Fraga, R.D. Pisarski, J. Schaffner-Bielich, Phys. Rev. D **63**, 121702 (2001).

[13] A. Peshier, B. Kämpfer, O.P. Pavlenko, G. Soff, Phys. Lett. B **337**, 235 (1994); Phys. Rev. D **54**, 2399 (1996); P. Levai, U. Heinz, Phys. Rev. C **57**, 1879 (1998).

[14] A. Peshier, B. Kämpfer, G. Soff, Phys. Rev. C **61**, 045203 (2000).

[15] F. Karsch, A. Patkos, P. Petreczky, Phys. Lett. B **401**, 69 (1997); A. Peshier, B. Kämpfer, O.P. Pavlenko, G. Soff, Europhys. Lett. **43**, 381 (1998); J.O. Anderson, E. Braaten, M. Strickland, Phys. Rev. Lett. **83**, 2139 (1999); Phys. Rev. D **61**, 014017 (2000); J.P. Blaizot, E. Iancu, A. Rebhan, Phys. Rev. Lett. **83**, 2906 (1999); Phys. Lett. B **470**, 181 (1999); Phys. Rev. D **63**, 065003 (2001); R. Baier, K. Redlich, Phys. Rev. Lett. **84**, 2100 (2000); A. Peshier, Phys. Rev. D **63**, 105004 (2001).

[16] F. Karsch, E. Laermann, A. Peikert, Phys. Lett. B **478**, 447 (2000).

[17] F. Karsch, hep-ph/0103314, Nucl. Phys. A in print.

[18] K. Rajagopal, F. Wilczek, hep-ph/0011333.

[19] K. Rajagopal, F. Wilczek, Phys. Rev. Lett. **86**, 3492 (2001).

[20] F. Karsch, E. Laermann, A. Peikert, hep-ph/0012023.

[21] C. Alcock et al., Astrophys. J. **542**, 281 (2000).

	fit 1	fit 2	fit 3
$N_f = 2$	[4.4, 0.73]	[6.0, 0.80]	[11.5, 0.90]
$N_f = 3$	[5.3, 0.73]	[7.8, 0.80]	[15.2, 0.88]

TABLE I. The parameters $[\lambda, -T_s/T_c]$ in the effective coupling (1), fitted to the lattice data [16].